

This discussion paper is/has been under review for the journal Atmospheric Measurement Techniques (AMT). Please refer to the corresponding final paper in AMT if available.

Particle-size distribution of polybrominated diphenyl ethers (PBDEs) and its implications for health

Y. Lyu¹, T. Xu¹, X. Li¹, T. Cheng¹, X. Yang¹, X. Sun², and J. Chen¹

¹Shanghai Key Laboratory of Atmospheric Particle Pollution and Prevention (LAP3), Department of Environmental Science & Engineering, Fudan University, Shanghai 200032, China

²Environment Research Institute, Shandong University, Jinan 250100, China

Received: 19 October 2015 – Accepted: 17 November 2015 – Published: 9 December 2015

Correspondence to: X. Li (lixiang@fudan.edu.cn) and X. Sun (xmwch@sdu.edu.cn)

Published by Copernicus Publications on behalf of the European Geosciences Union.

AMTD

8, 12955–12992, 2015

PBDEs size
distribution and
health impact

Y. Lyu et al.

Title Page

Abstract

Introduction

Conclusions

References

Tables

Figures

◀

▶

◀

▶

Back

Close

Full Screen / Esc

Printer-friendly Version

Interactive Discussion



Abstract

In order better to understand the particle-size distribution of particulate PBDEs and their deposition pattern in human respiratory tract, we made an one year campaign 2012–2013 for the measurement of size-resolved aerosol particles at Shanghai urban site. The results showed that particulate PBDEs exhibited a bimodal distribution with a mode peak in the accumulation particle size range and the second mode peak in the coarse particle size ranges. As the number of bromine atoms in the molecule increased, accumulation mode peak intensity increased while coarse mode peak intensity decreased. This change was the consistent with the variation of PBDEs' sub-cooled vapor pressure. Absorption and adsorption process dominated the distribution of PBDEs among the different size particles. Evaluated deposition flux of $\Sigma 13\text{PBDE}$ was 26.8 pg h^{-1} , in which coarse particles contributed most PBDEs in head and tracheobronchial regions, while fine mode particles contributed major PBDEs in the alveoli region. In associated with the fact that fine particles can penetrate deeper into the respiratory system, fine particle-bound highly brominated PBDEs can be inhaled more deeply into human lungs and cause a greater risk to human health.

1 Introduction

Polybrominated diphenyl ethers (PBDEs) are a class of organobromine compounds that are widely used as flame retardant. They are applied to a broad array of textiles and consumer products including plastics, polymers, mattresses, upholstery, carpeting, building materials and electronic equipment (de Wit, 2002; Alaee et al., 2003). Because the compounds are additive rather than chemically bound to the products, they can be released into the environment. They are persistent organic chemicals and can bioaccumulate, therefore, they have become contaminants detectable in the environment, in animals, and in humans (Su et al., 2009; Besis and Samara, 2012). Human uptake is thought to be through inhalation, dermal absorption and consumption of contaminated

AMTD

8, 12955–12992, 2015

[Title Page](#)

[Abstract](#)

[Introduction](#)

[Conclusions](#)

[References](#)

[Tables](#)

[Figures](#)

◀

▶

◀

▶

[Back](#)

[Close](#)

[Full Screen / Esc](#)

[Printer-friendly Version](#)

[Interactive Discussion](#)



food (Marklund et al., 2003; Wensing et al., 2005). The primary source of exposure to humans is believed to be consumption of contaminated fish, poultry, meat and dairy products (Su et al., 2009; Besis and Samara, 2012). Occupational exposures may occur in computer, electronic warehouses and formulation facilities (Harrad et al., 2010).
5 Inhalation exposure can take place through ambient aerosol or dust containing PBDEs. Compared with dust PBDEs, the inhalation of ambient aerosols may be a minor pathway for human people, but it has a long-term bioaccumulation process in human body. When PBDEs are suspended in air, they can be present as particles. Since we can not say how long PBDEs remain in the air, long-term exposure to PBDEs has a greater
10 potential to cause health effects than does short-term exposure to low levels because of their tendency to build up in your body over many years. Growing concerns about the health impacts of PBDEs have led to decline in their production and finally banned to use in the US and Europe since 2004 (Kemmlein et al., 2009). All technical mixtures of PBDEs were also totally phased out in other regions including China (Betts, 2008).
15 However, it is likely that long-term exposure will continue long after PBDE production has ended through emissions from PBDE-containing products that are still being used. Thus, it becomes necessary to investigate the particulate PBDEs characteristic existing in urban ambient aerosols.

Over the past decade, measurements on atmospheric PBDEs have been carried out
20 in various areas around the world such as Turkey (Cetin and Odabasi, 2008), Japan (Kakimoto et al., 2014), Thailand (Muenhor et al., 2010) and China (Yang et al., 2013) in Asia, USA (Hale et al., 2003) and Canada (Wilford et al., 2004) in North America, Greece (Besis et al., 2015), France (Castro-Jimenez et al., 2011) and Czech (Okonski et al., 2014) in Europe and someplace in Arctic (Moller et al., 2011; Wang et al., 2005).
25 In these studies, the particulate PBDEs were mainly investigated in the individual particle size fractions such as $PM_{2.5}$ and PM_{10} , and rarely involved with size-resolved particles. Particle-size distribution of PBDEs was crucial when evaluating human health risks since the size-resolved particles dominated deposition behavior of particles in the respiratory tract. To the best of our knowledge, particle-size distribution of PBDEs

PBDEs size distribution and health impact

Y. Lyu et al.

[Title Page](#)

[Abstract](#)

[Introduction](#)

[Conclusions](#)

[References](#)

[Tables](#)

[Figures](#)

◀

▶

◀

▶

[Back](#)

[Close](#)

[Full Screen / Esc](#)

[Printer-friendly Version](#)

[Interactive Discussion](#)



was merely reported in Thessaloniki, Athens (Greece) (Mandalakis et al., 2009; Besis et al., 2015), e-waste recycling sites in close to Guangzhou (China) (B. Z. Zhang et al., 2012; Luo et al., 2014b), and Brno (Czech) (Okonski et al., 2014). These studies showed that major lighter brominated congeners existed on coarse particles, while most highly brominated congeners occurred in fine particles. In association with the fact that fine particles can easily penetrate/enter the alveolar region, fine particle-bound highly brominated congeners can travel deep into the lungs and cause serious health problems for human people (Geiser et al., 2005). To clarify this issue we first need to investigate the actual particle-size distribution of PBDEs through a long-term observation.

This investigation was conducted in urban Shanghai with the aim to evaluate the contribution of particle-size distribution of PBDEs and their deposition in human respiratory tract. Besides this, the elucidation of influence of some factors such as the volatility, the chemical affinities and releasing source onto these distributions was also attempted.

15 2 Experimental and methods

2.1 Chemicals

Standard mixtures of PBDEs (BDE-17, -28, -47, -66, -71, -85, -99, -100, -138, -153, -154, -183, -190 and -209) were purchased from AccuStandard, Inc. (USA). Internal standards (¹³C-BDE-28, 47, 99 and 153) were purchased from Cambridge Isotope Laboratories (Andover, MA). PBDE congeners are divided into 5 groups (e.g., tri-, tetra-, penta-, hexa- and hepta-BDE) based on the number of bromine atoms in the molecule. The solvents used in this research were HPLC/spectro grade and bought from Tedia Company Inc. (USA).

[Title Page](#)

[Abstract](#)

[Introduction](#)

[Conclusions](#)

[References](#)

[Tables](#)

[Figures](#)

◀

▶

◀

▶

[Back](#)

[Close](#)

[Full Screen / Esc](#)

[Printer-friendly Version](#)

[Interactive Discussion](#)



2.2 Sample collection

The sampling campaign took place on the rooftop (20 m above the ground) of No. 4 teaching building at Fudan University campus (121.50° E, 31.30° N), approximately 5 km northeast of downtown Shanghai city (elevation about 4 m a.s.l.). A Fudan super monitoring station for atmospheric chemistry was running all year round. The site was in close proximity to digital malls, residences and the traffic around was busy due to close to sub-downtown. The main releasing sources at this site included industries emission, household heating and road transport. Details regarding the sampling site were included in our previous work (P. F. Li et al., 2011; X. Li et al., 2011). Particle samples were collected by drawing air through quartz fiber filter (Whatman QMA, ø81 mm), using an Anderson 8-stage air sampler (Tisch Environmental Inc., USA). The flow rate was controlled at 28.3 L min^{-1} . The cutoff aerodynamic diameters for each stage were < 0.4 , $0.4\text{--}0.7$, $0.7\text{--}1.1$, $1.1\text{--}2.1$, $2.1\text{--}3.3$, $3.3\text{--}4.7$, $4.7\text{--}5.8$, $5.8\text{--}9.0$ and $> 9.0 \mu\text{m}$. The whole observing period ranged from December 2012 to November 2013. The sampling time was 120 h for each sample batch. A total of 189 particle samples (21 sample batches containing 9 size fractions) were obtained at this site. Prior to sampling, the filters that wrapped in aluminum foils were baked at 450 °C for 12 h to remove organic materials. After sampling, loaded filters together with aluminum foils were stored at -20°C until extraction. In addition, meteorological data during the sampling period was obtained from the Fudan atmospheric monitoring station (Lv et al., 2015).

2.3 Sample extraction

The aerosol samples were extracted by Soxhlet with a mixture of dichloromethane/hexane (1 : 1, v/v). The extraction time was 36 h at a constant temperature 69°. After extraction, the samples were filtered through 0.45 μm PTFE syringe filters and concentrated using a rotary evaporator (BÜCHI Rotavapor, Switzerland) and a pure N_2 stream. Before instrumental analysis, ^{13}C -BDE-28, -47, -99 and 153 were added to the final extract as internal standards.

[Title Page](#)

[Abstract](#)

[Introduction](#)

[Conclusions](#)

[References](#)

[Tables](#)

[Figures](#)

◀

▶

◀

▶

[Back](#)

[Close](#)

[Full Screen / Esc](#)

[Printer-friendly Version](#)

[Interactive Discussion](#)



2.4 Instrumental analysis

Each compound was quantified by an Agilent 7890A Series GC coupled to an Agilent 7000B Triple Quadruple MS (GC/MS/MS, Agilent Technologies Inc., USA) operating at electron impact energy of 70 eV and using the Multiple Reaction Monitoring (MRM) mode. Samples separation was carried out by a DB-5MS (15 m × 0.25 mm i.d. with 0.25 µm film thickness) capillary column (J&W Scientific, Folsom, CA). The column temperature procedure was initially at 150 °C, then 12 °C min⁻¹ to 315 °C with 2 min hold. All samples were automatically injected by 2 µL in pluse splitless mode. The injector temperature was set to 330 °C, the transfer line to 310 °C and the ion trap to 300 °C. High-purity Helium (99.999 %) was applied as carrier gas with a constant flow rate of 1.2 mL min⁻¹ in column. Nitrogen gas was used as collision gas in MS. The identification and quantification of PBDEs were done according to retention times, selected precursor ions, product ions and the internal standard method relative to the closest eluting PBDE surrogate. The calibration solutions were prepared at five concentrations and contained uniform concentrations of the internal standards. For each analyte, a relative response factor was determined for each calibration level using the internal standard. The five response factors were then averaged to produce a mean relative response factor for each species. Reported analyte concentrations were corrected for internal standards recoveries. The calibration curves showed a linear response in the range 0.1–5 µg L⁻¹. The correlation coefficients of the calibration curve for the different PBDEs were $R^2 > 0.99$.

2.5 Quality control and assurance

Each batch of samples included one procedural blanks. In that case, only BDE-71, 100, 154 and 190 were commonly detected at much lower levels (< 5 %) in some samples. The mean values of blanks were then subtracted from measured values of each sample. Method recoveries determined by spiking the sampling process (five replicates) with a standard mixture of PBDEs ranged from 75 to 175 %. The recoveries of the

[Title Page](#)

[Abstract](#)

[Introduction](#)

[Conclusions](#)

[References](#)

[Tables](#)

[Figures](#)

◀

▶

◀

▶

[Back](#)

[Close](#)

[Full Screen / Esc](#)

[Printer-friendly Version](#)

[Interactive Discussion](#)



isotopically-labelled PBDEs internal standard were higher than 70 % for all the samples (refer to SRM 2585, NIST, Gaithersburg, MD). Repeatability was evaluated by performing four analyses of a standard PBDEs solution containing the above mentioned PBDEs and the surrogate standards in the same conditions. The relative standard deviations (RSD) of the relative response factors were below the 10 % for all PBDEs. The method detection (DL) and quantification limits (QL) were calculated as the concentrations equivalent to three and ten times the noise of the quantifier ion for a blank sample (DL ranged from 0.05 to 0.6 $\mu\text{g m}^{-3}$). For the purpose of statistical analysis, samples with concentrations under LOD were assigned concentrations equal to 0.5 LOD (Okonski et al., 2014).

2.6 Size-specific gas/particle partition

Two processes are commonly accepted for illustrating mechanisms of particle-gas partition, i.e., adsorption and absorption process. In the case of adsorption, it assumes that chemicals adsorb to active sites on the surface of the particle. The gas-particle partitioning coefficients ($K_{\text{p-ads}}$) during the adsorption process is described by (Pankow, 1987):

$$K_{\text{p-ads}} = \frac{N_s A_{\text{TSP}} T e^{(Q_L - Q_v)/RT}}{1600 \rho_L^\circ}, \quad (1)$$

where N_s is the surface concentration of sorption sites ($4 \times 10^{-10} \text{ mol cm}^{-2}$), A_{TSP} is the specific surface area of the particles, T is the ambient temperature (292 K), R is the ideal gas constant ($8.31 \text{ J mol}^{-1} \text{ K}^{-1}$), Q_L , Q_v are respectively the enthalpy of desorption from the surface and the enthalpy of vaporization of the subcooled liquid (kJ mol^{-1}), ρ_L° is the vapor pressure of the subcooled liquid. In contrast with PAHs, similar situation was assumed for PBDEs that $Q_L - Q_v \approx 1 \times 10^4 \text{ J mol}^{-1}$ (Aubin and Abbatt, 2006). After logarithmic transformation on both sides in Eq. (1), we can get the followed Eq. (2):

$$\log K_{\text{p-ads}} = -\log \rho_L^\circ + \log A_{\text{TSP}} - 8.35 \quad (2)$$

[Title Page](#)

[Abstract](#)

[Introduction](#)

[Conclusions](#)

[References](#)

[Tables](#)

[Figures](#)

[|◀](#)

[▶|](#)

[◀](#)

[▶](#)

[Back](#)

[Close](#)

[Full Screen / Esc](#)

[Printer-friendly Version](#)

[Interactive Discussion](#)



Size dependent A_{TSP} adopted from the results of Yu and Yu (2012) and the data was list in Table 2. Based on three modes, we then obtained Eq. (3) which derived from Eq. (2).

$$\log K_{p\text{-ads}} = \begin{cases} -\log p_L^\circ - 6.64 & \text{(Aitken mode: } < 0.4 \mu\text{m)} \\ -\log p_L^\circ - 7.25 & \text{(Accumulation mode: } 0.4 - 2.1 \mu\text{m)} \\ -\log p_L^\circ - 7.06 & \text{(Coarse mode: } 2.1 - 10 \mu\text{m)} \end{cases} \quad (3)$$

5 The temperature dependent p_L° values of PBDE congeners was calculated using the regression parameters by ($\log p_L^\circ = A + B/T$) (Tittlemier et al., 2002). In our study, the average temperature of sampling campaign was 292 K. The temperature dependent $\log p_L^\circ$ was list in Table 1.

10 In the case of absorption, it assumes that atmospheric aerosols are coated with an organic film and chemicals can absorb into this organic phase. The gas-particle partitioning coefficients ($K_{p\text{-abs}}$) during the absorption process is described by Finizio et al. (1997):

$$K_{p\text{-abs}} = 10^{-9} \frac{M_o \gamma_o}{M_{OM} \gamma_{OM} \rho_{OM}} f_{OM} K_{OA}, \quad (4)$$

15 where M_o and M_{OM} are the mean molecular weights of octanol and the organic matter phase (g mol^{-1}), γ_o and γ_{OM} are the activity coefficients of the absorbing compound in octanol and in the organic matter phase, respectively. f_{OM} is the fraction of organic matter phase on particles, K_{OA} is octanol-air partition coefficient. ρ_{OM} is the density of octanol (820 kg m^{-3} at 20°).

20 With the assumption that $\frac{M_o}{M_{OM}} = 1$, $\frac{\gamma_o}{\gamma_{OM}} = 1$, the Eq. (4) can be simplified to Eq. (5) after logarithmic transformation on both sides:

$$\log K_{p\text{-abs}} = \log K_{OA} + \log f_{OM} - 11.91 \quad (5)$$

Title Page

Abstract

Introduction

Conclusions

References

Tables

Figures

|◀

▶|

◀

▶

Back

Close

Full Screen / Esc

Printer-friendly Version

Interactive Discussion



Size-specific f_{OM} was adopted from Yu and Yu (2012) and list in Table 2. Through calculation, we can deduce Eq. (6) as followed:

$$\log K_{\text{p-abs}} = \begin{cases} \log K_{\text{OA}} - 12.26 & (\text{Aitken mode: } < 0.4 \mu\text{m}) \\ \log K_{\text{OA}} - 12.42 & (\text{Accumulation mode: } 0.4 - 2.1 \mu\text{m}) \\ \log K_{\text{OA}} - 12.51 & (\text{Coarse mode: } 2.1 - 10 \mu\text{m}) \end{cases} \quad (6)$$

K_{OA} has been reported as functions of temperature ($\log K_{\text{OA}} = A + B/T$) (Harner and Shoeib, 2002). In this study, the average temperature of sampling campaign was 292 K. The temperature dependent $\log K_{\text{OA}}$ was list in Table 1, along with other physiochemical properties of the target PBDE congeners.

Pankow (Pankow, 1994a) proposed a definition of the measured particle-gas partition coefficient ($K_{\text{p-measured}}$) to characterize the partitioning behavior of semi-volatile organic compounds (SVOCs) between the gas and particulate phases

$$K_{\text{p-measured}} = (P/\text{TSP}) / G \quad (7)$$

Where P and G are PBDEs in particulate and gas phase concentration, respectively, and TSP is the total suspended particulate ($\mu\text{g m}^{-3}$). After linear regression between $\log K_{\text{p-measured}} \sim \log p_{\text{L}}^{\circ}$ and $\log K_{\text{p-measured}} \sim \log K_{\text{OA}}$, we can get the relationship between $\log K_{\text{p-measured}} \sim \log p_{\text{L}}^{\circ}$ and $K_{\text{p-measured}} \sim \log K_{\text{OA}}$.

In association with Eqs. (4), (6) and (7), we can investigate the sorption mechanisms governing particle-size distribution of PBDEs by comparing theoretical $K_{\text{p-ads}}$ and $K_{\text{p-abs}}$ with measured $K_{\text{p-measured}}$.

2.7 Human respiratory risk assessment

Because the size-resolved particles played a key role in health risk assessment through inhalation (Luo et al., 2014a), we adopted a so-called International Commission on Radiological Protection (ICRP) model (International Commission on Radiological Protection, 1995) to evaluate the deposition efficiencies and fluxes of inhaled PBDEs in the

[Title Page](#)[Abstract](#)[Introduction](#)[Conclusions](#)[References](#)[Tables](#)[Figures](#)[◀](#)[▶](#)[◀](#)[▶](#)[Back](#)[Close](#)[Full Screen / Esc](#)[Printer-friendly Version](#)[Interactive Discussion](#)

human respiratory tract. The human respiratory tract can be divided into three regions: head airway (HA), tracheobronchial region (TB), and alveoli region (AR). The particle deposition efficiency (DE) in HA, TB and AR are estimated by the followed simplified Eqs. (8), (9) and (10):

$$DE_{HA} = IF \times \left[\frac{1}{1 + e^{6.84 + 1.183 \ln D_p}} + \frac{1}{1 + e^{0.924 - 1.885 \ln D_p}} \right] \quad (8)$$

$$DE_{TB} = \left(\frac{3.52 \times 10^{-3}}{D_p} \right) \times \left[e^{-0.234(\ln D_p + 3.40)^2} + 63.9 \times e^{-0.819(\ln D_p - 1.61)^2} \right] \quad (9)$$

$$DE_{AR} = \left(\frac{0.0155}{D_p} \right) \times \left[e^{-0.416(\ln D_p + 2.84)^2} + 19.11 \times e^{-0.482(\ln D_p - 1.362)^2} \right] \quad (10)$$

Where D_p is diameter of the particle, and IF is inhalable fraction of all particles,

$$IF = 1 - \left(1 - \frac{1}{1 + 7.6D_p^{2.8} \times 10^{-4}} \right) / 2.$$

The deposition flux (DF, pg h^{-1}) of inhaled particulate PBDEs in respiratory tract is estimated by

$$DF = \sum (DE_i \times C_i) \times V \quad (11)$$

Where DE_i is the particle deposition efficiency in each region for D_p (the average diameter of each particle size fraction); C_i is PBDEs concentration in particle D_p (pg m^{-3}); and V is the breathing rate. The lower and upper limit diameters of particles in this research were assumed to be 0.1 and 30 μm , respectively. The respiration rate under normal conditions was considered as $0.45 \text{ m}^3 \text{ h}^{-1}$ (K. Zhang et al., 2012).

In addition, we applied hazard quotient (HQ) values to assess non-cancer risk of size-resolved PBDEs through inhalation. The formula is as follows:

$$HQ = DI / (BW \times RfD), \quad (12)$$

[Title Page](#)

[Abstract](#)

[Introduction](#)

[Conclusions](#)

[References](#)

[Tables](#)

[Figures](#)

◀

▶

◀

▶

[Back](#)

[Close](#)

[Full Screen / Esc](#)

[Printer-friendly Version](#)

[Interactive Discussion](#)



where DI is daily intake (pg day^{-1}) and calculated by multiplying deposition flux (DF: pg h^{-1}) with average exposure time (ET: h day^{-1}), BW is mean body weight of adult (60 kg) and RfD is reported oral reference dose for PBDEs ($\text{pg kg}^{-1} \text{ bw day}^{-1}$).

In order to understand the impact of risk and uncertainty in size-resolved particles,
5 we used Monte Carlo simulations to produce probability distributions of hazard levels with five thousand trials. Moreover, we used the SPSS version 22.0 (IBM company, Chicago, IL, USA) to perform Pearson correlation analysis for all data and considered p values of smaller than 0.01 or 0.05 statistically significant.

3 Results and discussion

10 3.1 PBDEs occurrence and seasonal variation

Most PBDE congeners were detected in the vast majority of samples (Fig. 1 and Table 3). BDE-71, 100, 154 and 190 were sometimes present close to the detection limits of the method. Due to the erratic concentration of BDE 209, this compound has been removed from further analysis. The box plot in Fig. 1 summarizes the concentrations measured throughout the year and allows for easy visualization of PBDE congener groups (e.g., tri-, tetra-, penta-, hexa- and hepta-BDEs). The box contains the middle 50 % of the data, whereas the top and bottom end of the box represent the 75th and 25th percentiles of the data set, respectively. The extensions ("whiskers") at either end of the box indicate the 95 and 5 percentile and the solid spheres represent the maximum and minimum values. The median concentrations are indicated by the solid vertical lines whereas the mean concentrations are depicted by the horizontal line. In general, the size of the box and the length of the whiskers are an indicator of the variability in concentrations at a given site for a given compounds containing the same number of bromine atoms. A small box shows that the distribution is uniform over the entire sampling period and vice versa. In these groups, penta-BDEs ($49.5 \pm 21.5 \text{ pg m}^{-3}$) were the dominant congeners detected in all sam-

[Title Page](#)

[Abstract](#)

[Introduction](#)

[Conclusions](#)

[References](#)

[Tables](#)

[Figures](#)

◀

▶

◀

▶

[Back](#)

[Close](#)

[Full Screen / Esc](#)

[Printer-friendly Version](#)

[Interactive Discussion](#)





bles, followed by hexa-BDE ($16.7 \pm 7.8 \text{ pg m}^{-3}$), hepta-BDE ($11.2 \pm 3.1 \text{ pg m}^{-3}$), tetra-BDE ($5.9 \pm 1.3 \text{ pg m}^{-3}$) and tri-BDE ($1.3 \pm 0.3 \text{ pg m}^{-3}$). Among individual PBDEs, PBDE-47, -99 and -85 were detected in 100 % of the ambient aerosol samples, with BDE-99 and -85 being the most dominant congeners. This may be due to the fact that less brominated BDEs have longer half-lives (years) and could be formed through debromination of more brominated congeners (Bezares-Cruz et al., 2004). The observed average concentrations of particulate $\Sigma 13\text{PBDEs}$ were ranged from 30.6 to 141.2 pg m^{-3} with a mean value of 86.3 pg m^{-3} (Table 3). This result was consistent with the results of the previous measurements in Shanghai $108\text{--}367 \text{ pg m}^{-3}$ (Yang et al., 2013) and $104 \pm 54 \text{ pg m}^{-3}$ (Yu et al., 2011), but was much lower than in Beijing 760 pg m^{-3} (Yang et al., 2013) and in waste recycling zones of Qingyuan close to Guangzhou 3260 pg m^{-3} (Tian et al., 2011). In addition, this results were compared with those reported in aerosol samples from Ontario $88\text{--}1250 \text{ pg m}^{-3}$ (Gouin et al., 2012), Chicago $100 \pm 35 \text{ pg m}^{-3}$ (Hoh and Hites, 2005) and three different stations in western Europe $0.22\text{--}37 \text{ pg m}^{-3}$ (Lee et al., 2004), as well as other Asian cities such as Osaka ($9.9\text{--}22.3 \text{ pg m}^{-3}$) (Kakimoto et al., 2014), Busan ($5.3\text{--}16 \text{ pg m}^{-3}$), (Rudich et al., 2007) and Singapore (7.5 pg m^{-3}) (Shen et al., 2013). These direct comparison of PBDEs concentrations between various urban environments should be done with caution. Because of the differences existing within any urban environment, PBDE levels could be significantly affected by the location of the sampling site and its proximity to emission sources. Moreover, sampling methodology is a critical parameter affecting the comparison between the observed concentrations of PBDEs in different sites. In most published studies, collection of particulate PBDEs has been performed by using different sampling, pretreatment and instrumental analysis system devices and in some cases underestimation of PBDE concentrations might have occurred because more volatile species were mainly in the gas phase and easy to be lost during membrane sampling or storage period.

Seasonal variations were distinct at this urban sites, with significantly higher concentrations measured during winter (104–141 pg m^{-3}) and lower concentrations measured

5 during summer (30.6–82.2 pg m^{-3}) (Table 3). Higher concentrations in winter were at least in part due to increased emissions and by the distinctive meteorological conditions including reduced mixing heights and lower precipitation depth for favoring the pollutants accumulation in the atmosphere (Volckens and Leith, 2003). In addition, the adsorption of gaseous PBDEs on particles was likely to increase during winter since the partition coefficient, K_p was inversely correlated with temperature ($r = -0.867$, $p < 0.01$) (see Fig. 2). Lower concentrations in summer may have been caused by wet scavenging since some summer sampling days experienced precipitation at this site. Seasonal variations in PBDEs can also be explained by the Asian monsoon patterns. Shanghai sites are situated in a transitional zone of the northern subtropical monsoon system, where the northwesterly winter monsoon bring polluted air masses from China Mainland, while the southeasterly summer monsoon bring cleaner oceanic aerosols comes from the oceans (Western Pacific) (Shi and Cui, 2012). Moreover, higher wind speeds appeared to be typically associated with lower PBDEs concentrations ($r = -0.583$, $p < 0.01$) (Fig. 2). Higher PBDEs concentrations were associated with higher $\text{PM}_{2.5}$ level ($r = 0.629$, $p < 0.01$) and lower visibility ($r = -0.686$, $p < 0.01$). This seasonal pattern were consistent with those measured in Huaniao Island (Li et al., 2015), Qingyuan (Tian et al., 2011) and Dongguan (Zhang et al., 2009).

3.2 PBDEs size distribution and process mechanism

20 Among the PBDE congeners measured, we chose BDE-47, -85, -99, -138, -153 and -183 for the study on size distribution due to detection frequencies higher than other congeners. Figure 3 plots the average size distributions of these PBDEs in the continuous smoothed curves inverted from the sample data. The results showed that particulate PBDEs exhibited a bimodal distribution with a mode peak in the accumulation 25 particle size range and the second mode peak in the coarse particle size ranges. As the number of bromine atoms in the molecule increased, accumulation mode peak intensity increased while coarse mode peak intensity decreased, which indicated that the lighter

PBDEs size distribution and health impact

Y. Lyu et al.

[Title Page](#)

[Abstract](#)

[Introduction](#)

[Conclusions](#)

[References](#)

[Tables](#)

[Figures](#)

◀

▶

◀

▶

[Back](#)

[Close](#)

[Full Screen / Esc](#)

[Printer-friendly Version](#)

[Interactive Discussion](#)



5 brominated congeners BDE 47 and 85 were mainly associated with particles larger than 2.1 mm, whereas the highly brominated congeners were mainly sorbed to the fine particles. The similar bimodal distribution of PBDEs also occurred in Heraklion (Mandalakis et al., 2009), Brno and Telnice (Okonski et al., 2014), Guangzhou (B. Z. Zhang et al., 2012). Differences in the particle-size distribution of individual PBDEs could reflect differences in their emission sources but there was no credible scientific evidence in support of this claim. Although published data on particle-size distribution of PBDEs are not available for comparison, analogous trends have also been observed for other classes of organic contaminants such as PAHs. Previous field measurements by 10 cascade impactors demonstrated that more-ring PAHs were sorbed to the fine aerosol fraction, while more volatile or low-ring species were associated with larger particles (Wang et al., 2015; Kavouras et al., 1999; Kawanaka et al., 2004; Bi et al., 2005). The reason on these is due to the different volatility of PAHs, since more volatile species are absorbed to fine aerosol and distribute in coarse particles by rapid volatilization 15 and condensation. On the contrary, for the more-ring PAHs, due to the lower vapour pressures, the time required for this repartitioning process is much longer (Bi et al., 2005), therefore, they tend to remain in fine particles initially emitted (Duan et al., 2007). This hypothesis can explain the relatively higher abundance of more volatile PAHs in the coarse particle mode. Similarly, it can be applied the particle-size distribution 20 of PBDEs. To further confirm this hypothesis, the geometric mass diameter (GMD) for particulate PBDEs was calculated and correlated with logarithmic subcooled liquid vapor pressures ($\log P_L$) (Fig. 4). The mean GMD values for all PBDE congeners was ranged from 1.9 to 2.9 μm in Shanghai, which was higher than those in Greece (0.14–0.63 μm) (Mandalakis et al., 2009) and Guangzhou (0.98–1.98 μm) (Luo et al., 2014b). 25 Moreover, there are a positive moderate correlation between GMD and $\log P_L$ ($r = 0.69$, $p < 0.01$), indicating the GMD increases as the volatile of PBDE congeners increases. This phenomenon becomes more apparent in coarse size fraction with a increased positive correlation ($r = 0.75$, $p < 0.01$) (right panel in Fig. 4). This result suggests that most coarse particle-bound PBDEs contain higher volatile species such as tri- and

PBDEs size distribution and health impact

Y. Lyu et al.

[Title Page](#)[Abstract](#)[Introduction](#)[Conclusions](#)[References](#)[Tables](#)[Figures](#)[◀](#)[▶](#)[◀](#)[▶](#)[Back](#)[Close](#)[Full Screen / Esc](#)[Printer-friendly Version](#)[Interactive Discussion](#)

tetra-BDEs. They are derived from the secondary distribution process, i.e., re-volatilize from fine particles and re-condensate onto coarse ones (Wang et al., 2008; La Guardia et al., 2006).

Moreover, chemical affinities also played an important role in PBDEs' distribution process. Theoretically, highly brominated congeners had strong hydrophobicity and prefer to bound with small particles because they had large surface areas (Venkataraman et al., 1999). Such an explanation, however, cannot adequately account for the PBDEs distribution patterns observed in the present study. Perhaps in fact other factors, e.g. emission sources, sampling sites and weather conditions (temperature and/or relative humidity) might also influence their distributions (Zielinska et al., 2004). Although there were still difficulties in totally clarifying the size distributing mechanism of PBDEs or other SVOCs now, it was important to integrate all factors in consideration in future study.

3.3 Preliminary study on PBDEs partitioning mechanisms

Usually, two major mechanisms, i.e., adsorption and absorption played the important role in PBDEs partitioning to multimodal urban aerosols (Lohmann and Lammel, 2004). To clarify these processes, the theoretical $K_{p\text{-ads}}$ and $K_{p\text{-abs}}$ were respectively calculated based on Eqs. (3) and (6) because they involved the size-specific parameters, usually including organic matter fractions and the available adsorptive sites on aerosol particles (Pandis et al., 1992; Pankow, 1994b). The obtained theoretical $K_{p\text{-ads}}$ and $K_{p\text{-abs}}$ values were estimated and compared with measured $K_{p\text{-measured}}$ (from Eq. 7). Since we had no gas PBDEs concentrations, the measured $K_{p\text{-measured}}$ were based on a recent study in shanghai by Yang et al. (2013). In their studies, both gas and particulate PBDEs concentration were reported at an urban site about ~ 50 km away from our site (Table 1). A range of $10\text{--}70 \mu\text{g m}^{-3}$ was assumed for size-specific particle concentration to calculate $K_{p\text{-measured}}$. The measurement periods ranged from September 2008 to August 2009. The average temperature was 18.4°C , similar to the temperatures in our study (19°C). Therefore, their data could serve as useful reference for us to compare

Title Page

Abstract

Introduction

Conclusions

References

Tables

Figures

|◀

▶|

◀

▶

Back

Close

Full Screen / Esc

Printer-friendly Version

Interactive Discussion



with the theoretical $K_{p\text{-ads}}$ and $K_{p\text{-abs}}$ derived from adsorption and absorption in our study. Note that we took $< 0.4\mu\text{m}$, $0.4\text{--}2.1\mu\text{m}$ and $> 2.1\mu\text{m}$ for Aitken, accumulation and coarse mode, respectively.

The plots of measured $\log K_{p\text{-measured}}$ vs. $\log p_L^\circ$ and $\log K_{\text{OA}}$ were presented in Fig. 5, along with two sets of theoretical $K_{p\text{-ads}}$ and $K_{p\text{-abs}}$ based on adsorption and absorption in three modes. As presented, significant linear correlations were found between measured $\log K_{p\text{-measured}}$ and $\log p_L^\circ$ ($R^2 = 0.76$) as well as measured $\log K_{p\text{-measured}}$ and $\log K_{\text{OA}}$ ($R^2 = 0.77$). For the same class compounds under equilibrium conditions by either adsorption or absorption, the slope of log-log plots of K_p and p_L° was expected to be close to -1 (Pankow and Bidleman, 1992) and the slope of log-log plots of K_p and K_{OA} should be close to 1 (Finizio et al., 1997). However, more gentle regression lines (slopes: -0.53 , 0.68) were detected (Fig. 5), similar to slopes reported in previous studies (Cetin and Odabasi, 2008; Yang et al., 2012). The deviations were possibly caused by kinetic limitations (non-equilibrium partition), thermodynamic limitations (lack of constancy in desorption) and additional sorption (Harner and Bidleman, 1998; Cousins and Mackay, 2001; Lohmann et al., 2007).

The three mode data sets of theoretical $\log K_{p\text{-ads}}$ and $\log K_{p\text{-abs}}$ in Fig. 5a and b were calculated using Eqs. (3) and (6), considering only adsorption mechanism or absorption mechanism, respectively. As expected, the slopes for them were all -1 . Both $\log K_{p\text{-ads}}$ considering only adsorption and $\log K_{p\text{-abs}}$ considering only absorption were compared with measured $\log K_{p\text{-measured}}$ in Fig. 5. The results showed that the $K_{p\text{-measured}}$ values of highly brominated congeners (e.g., BDE-85, -99, -100, -138, -153, -154 and -183) in three modes fell into the regression line of the theoretical $K_{p\text{-ads}}$ (Fig. 5a), while the measured $K_{p\text{-measured}}$ values of lighter brominated congeners (e.g., BDE-17, -28, -47 and -66) in three modes fell into the regression line of the theoretical $K_{p\text{-abs}}$ (Fig. 5b). These facts revealed that adsorption on surfaces of particles appeared to be responsible for bimodal distribution of highly brominated congeners, while absorption into organic matter seemed to play an important role for lighter brominated congeners. In addition, we can find the measured $K_{p\text{-measured}}$ lines are respec-

Title Page

Abstract

Introduction

Conclusions

References

Tables

Figures

|◀

▶|

◀

▶

Back

Close

Full Screen / Esc

Printer-friendly Version

Interactive Discussion



10 **3.4 Correlation analysis of PBDEs**

Table 4 presents a Pearson correlation matrix among PBDE congeners based on concentrations. Significant correlation was found among the tri-BDEs (BDE-17 and -28, $r = 0.75$, $p < 0.05$), as well as penta-BDEs (BDE-100, -99 and -85, $r = 0.67$ – 0.83 , $p < 0.05$). These high correlation values suggested tri-BDEs and/or penta-BDEs shared a common source and/or exhibited a similar distribution behavior in environment. BDE-28 significantly correlated with BDE-71 ($r = 0.65$, $p < 0.05$), and both of them also significantly correlated with penta-BDEs 100, 99 and 85. As we known, penta-BDEs were frequently detected in ambient particles around solid waste incineration plants (Dong et al., 2015). In this observation, we also found that penta-BDEs appeared high concentrations (mean: 49.5 pg m^{-3}) compared with other congeners. Thus, we concluded that these penta-BDEs and correlated congeners probable came from the same source regions because there were numerous of solid waste incineration plants located in surrounding places of Shanghai. Hepta-BDE (BDE-183 and -190) correlated poorly with the other congeners, with only two exception, which were statistically significant at the $r = 0.47$, $p < 0.01$ level for BDE-183 and -138, as well as $r = 0.71$, $p < 0.05$ level for BDE-190 and -47, respectively. This suggested hepta-BDEs might not originate from same sources. Other studies showed there existed possibilities of decomposition of higher brominated PBDEs to form lower brominated PBDEs in atmosphere (Eriksson

Title Page	
Abstract	Introduction
Conclusions	References
Tables	Figures
◀	▶
◀	▶
Back	Close
Full Screen / Esc	
Printer-friendly Version	
Interactive Discussion	



et al., 2004; Söderström et al., 2004; Kajiwara et al., 2008). Here we did not measure higher brominated PBDEs (octa- and deca-BDEs) and no correlation analysis were performed on them. But as seen in Fig. 1, the hexa- vs. hepta-BDEs concentrations (mean: 16.7 and 11.2 pg m^{-3}) were relatively high, thus indicative of multiple releasing sources in this area, i.e., local emission, higher brominated PBDEs breakdown and long-range atmospheric transport maybe had the potential contributions to hexa- and hepta-BDEs contaminations.

3.5 Implication for health

In this section, we calculated the regional deposition flux in human respiratory tract based on Eqs. (8), (9) and (10). Figure 6 showed the deposition fluxes of size-resolved PBDEs for adult men. The total deposition fluxes of $\Sigma 13\text{PBDE}$ were calculated at 26.8 pg h^{-1} . Among these compounds, penta-BDE was the major congeners and contributed a mean value of 58 % (range: 31–70 %) to the total deposition fluxes. The percent contribution of $\Sigma 13\text{PBDEs}$ to the respiratory tract were 84.4 % (22.64 ng h^{-1}) in the head airway, 4.6 % (1.24 ng h^{-1}) in the tracheobronchial, and 11.0 % (2.93 pg h^{-1}) in the alveoli regions, respectively. Moreover, we also found that coarse particles contributed major PBDEs in the head and tracheobronchial regions, while fine particles (accumulation plus Aitken mode particles) contributed lots of PBDEs in the alveoli region. As we known, the particle-size distribution of PBDEs has a decisive influence on their potential health effects. Considering that fine particles can penetrate deeper into the respiratory system compared to coarse particles, fine particle-bound PBDEs are expected to accumulate in the lower parts of the lungs and pose a greater risk to human health.

We further evaluated the human health risk that caused by PBDEs by using HQ approach based on inhaled PBDEs data. Figure 7 showed that the HQ values of the individual congeners were ranging from 4.0×10^{-7} to 6.8×10^{-5} with the total value of 1.6×10^{-4} for $\Sigma 13\text{PBDE}$. During the assessment process, we found that the HQ values was highly dependent on the variable daily intake (DI, see Eq. 12), which was incon-

Title Page

Abstract

Introduction

Conclusions

References

Tables

Figures

|◀

▶|

◀

▶

Back

Close

Full Screen / Esc

Printer-friendly Version

Interactive Discussion



stant and would result in uncertainty in the risk evaluation. Taking these situations into consideration, we utilized Monte Carlo (MC) simulation to evaluate the influences of uncertainty on this exposure model and to examine whether a difference exists between the model and the calculated HQ. In the simulation, the MC procedure was repeated 5 5000 times with different calculated HQ. The results of the simulation were depicted in Fig. 8, which exhibited a wide gamma distribution. The 95 % percentile values of HQ were in the range 9.15×10^{-5} – 8.36×10^{-5} , with the mean value of 8.76×10^{-5} . In comparison with the corresponding experimental HQ data (1.6×10^{-4}), excellent agreements could be observed between the data, indicating the accuracy of our simulation.

10 By comparison, these HQ values in the present study were much lower than the risk guideline value (1.0) recommended by the US EPA. Even under heavy exercise conditions (assuming a high breathing rate of $3 \text{ m}^3 \text{ h}^{-1}$), the estimated HQ of $\Sigma 13\text{PBDE}$ was only $(1.17 \pm 0.42) \times 10^{-3}$, far less than 1. Thus, particulate PBDEs in Shanghai urban atmosphere posed low noncancer risk through inhalation. However, it was noteworthy 15 here that only particle phase PBDEs participated in the assessment and we were not sure whether the risk posed by atmospheric PBDEs (gas plus particle) exceeded the threshold. Specifically, BDE-47 and BDE-99 mainly existed in gas phase, were probably more toxic and bioaccumulative than other congeners (Darnerud, 2003). Furthermore, we only measured 13 PBDE congeners, neglecting risk caused by substantial octa -

20 BDE and deca -BDE in particles, and other ways of exposure like ingestion, dermal contact were not considered, either. Thus, it was not to suggest that the occurrence of particulate PBDEs in shanghai was not an issue; rather, we advocated further studies that measuring of more PBDE congeners in not only particle phase but gas phase in relation to health risk assessment.

25 4 Summary and conclusions

This study revealed the particle-size distribution of PBDEs in the Shanghai urban atmosphere and calculated the contribution of each size-specific particle to PBDEs deposit-

Title Page	
Abstract	Introduction
Conclusions	References
Tables	Figures
◀	▶
◀	▶
Back	Close
Full Screen / Esc	
Printer-friendly Version	
Interactive Discussion	



ing in respiratory tract. The particle-size distribution of PBDEs were bimodal distribution with one peak at fine size fractions and the second peak at coarse size fractions. The peaks intensities were associated the molecular weights of PBDEs. The possible reasons were expounded by the parameters such as physicochemical properties of PBDEs, meteorological factors and the emission source. Adsorption and absorption mechanisms respectively played the crucial roles in highly and lightly brominated congeners. Most PBDEs were predominantly distributed in small particles, which contributed the majority of PBDEs deposition fluxes in the human respiratory tract. Total deposition fluxes of target Σ 13PBDE in the respiratory tract was calculated at 26.8 ng h^{-1} .

5 The non-cancer risk of PBDEs from inhaling particles in Shanghai urban atmosphere showed somewhat low. Further studies will be focused on the investigations of fine or ultrafine particles as transporters of toxic compounds from the atmosphere to the respiratory tract, and the evaluations of exposure risks to ultrafine particles in the atmosphere.

10

15 *Acknowledgements.* This work was supported by the National Natural Science Foundation of China (Nos. 21577021, 21177025, 21377028, 21277082, 41475109), the Excellent Academic Leader Program (No. 14XD1400600), FP720 project (AMIS, IRSES-GA-2011) and the program for New Century Excellent Talents in University (NCET-13-0349).

References

20 Alae, M., Arias, P., Sjodin, A., and Bergman, A.: An overview of commercially used brominated flame retardants, their applications, their use patterns in different countries/regions and possible modes of release, *Environ. Int.*, 29, 683–689, 2003.

Aubin, D. G. and Abbatt, J. P.: Laboratory measurements of thermodynamics of adsorption of small aromatic gases to *n*-hexane soot surfaces, *Environ. Sci. Technol.*, 40, 179–187, 2006.

25 Besis, A. and Samara, C.: Polybrominated diphenyl ethers (PBDEs) in the indoor and outdoor environments—a review on occurrence and human exposure, *Environ. Pollut.*, 169, 217–229, 2012.

[Title Page](#)

[Abstract](#)

[Introduction](#)

[Conclusions](#)

[References](#)

[Tables](#)

[Figures](#)

◀

▶

◀

▶

[Back](#)

[Close](#)

[Full Screen / Esc](#)

[Printer-friendly Version](#)

[Interactive Discussion](#)



Besis, A., Botsaropoulou, E., Voutsas, D., and Samara, C.: Particle-size distribution of polybrominated diphenyl ethers (PBDEs) in the urban agglomeration of Thessaloniki, northern Greece, *Atmos. Environ.*, 104, 176–185, 2015.

5 Betts, K. S.: Unwelcome guest: PBDEs in indoor dust, *Environ. Health Perspect.*, 116, A202–A208, 2008.

Bezares-Cruz, J., Jafvert, C. T., and Hua, I.: Solar photodecomposition of decabromodiphenyl ether: products and quantum yield, *Environ. Sci. Technol.*, 38, 4149–4156, 2004.

10 Bi, X., Sheng, G., Peng, P. A., Chen, Y., and Fu, J.: Size distribution of *n*-alkanes and polycyclic aromatic hydrocarbons (PAHs) in urban and rural atmospheres of Guangzhou, China, *Atmos. Environ.*, 39, 477–487, 2005.

Castro-Jimenez, J., Mariani, G., Vives, I., Skejo, H., Umlauf, G., Zaldivar, J. M., Dueri, S., Messiaen, G., and Laugier, T.: Atmospheric concentrations, occurrence and deposition of persistent organic pollutants (POPs) in a Mediterranean coastal site (Etang de Thau, France), *Environ. Pollut.*, 159, 1948–1956, 2011.

15 Cetin, B. and Odabasi, M.: Atmospheric concentrations and phase partitioning of polybrominated diphenyl ethers (PBDEs) in Izmir, Turkey, *Chemosphere*, 71, 1067–1078, 2008.

Cousins, I. T. and Mackay, D.: Gas–particle partitioning of organic compounds and its interpretation using relative solubilities, *Environ. Sci. Technol.*, 35, 643–647, 2001.

Darnerud, P. O.: Toxic effects of brominated flame retardants in man and in wildlife, *Environ. 20 Int.*, 29, 841–853, 2003.

de Wit, C. A.: An overview of brominated flame retardants in the environment, *Chemosphere*, 46, 583–624, 2002.

25 Dong, Y., Fu, S., Zhang, Y., Nie, H., and Li, Z.: Polybrominated diphenyl ethers in atmosphere from three different typical industrial areas in Beijing, China, *Chemosphere*, 123, 33–42, 2015.

Duan, J. C., Bi, X. H., Tan, J. H., Sheng, G. Y., and Fu, J. M.: Seasonal variation on size distribution and concentration of PAHs in Guangzhou city, China, *Chemosphere*, 67, 614–622, 2007.

30 Eriksson, J., Green, N., Marsh, G., and Bergman, A.: Photochemical decomposition of 15 polybrominated diphenyl ether congeners in methanol/water, *Environ. Sci. Technol.*, 38, 3119–3125, 2004.

PBDEs size distribution and health impact

Y. Lyu et al.

[Title Page](#)[Abstract](#)[Introduction](#)[Conclusions](#)[References](#)[Tables](#)[Figures](#)[|◀](#)[▶|](#)[◀](#)[▶](#)[Back](#)[Close](#)[Full Screen / Esc](#)[Printer-friendly Version](#)[Interactive Discussion](#)

PBDEs size distribution and health impact

Y. Lyu et al.

Finizio, A., Mackay, D., Bidleman, T., and Harner, T.: Octanol-air partition coefficient as a predictor of partitioning of semi-volatile organic chemicals to aerosols, *Atmos. Environ.*, 31, 2289–2296, 1997.

5 Geiser, M., Rothen-Rutishauser, B., Kapp, N., Schurch, S., Kreyling, W., Schulz, H., Semmler, M., Hof, V. I., Heyder, J., and Gehr, P.: Ultrafine particles cross cellular membranes by nonphagocytic mechanisms in lungs and in cultured cells, *Environ. Health Perspect.*, 113, 1555–1560, 2005.

10 Gouin, T., Thomas, G. O., Cousins, I., Barber, J., Mackay, D., and Jones, K. C.: Air-surface exchange of polybrominated biphenyl ethers and polychlorinated biphenyls, *Environ. Sci. Technol.*, 36, 1426–1434, 2002.

Hale, R. C., Alaee, M., Manchester-Neesvig, J. B., Stapleton, H. M., and Ikonomou, M. G.: Polybrominated diphenyl ether flame retardants in the North American environment, *Environ. Int.*, 29, 771–779, 2003.

15 Harner, T. and Bidleman, T. F.: Octanol-air partition coefficient for describing particle/gas partitioning of aromatic compounds in urban air, *Environ. Sci. Technol.*, 32, 1494–1502, 1998.

Harner, T. and Shoeib, M.: Measurements of octanol-air partition coefficients (K-OA) for polybrominated diphenyl ethers (PBDEs): predicting partitioning in the environment, *J. Chem. Eng. Data*, 47, 228–232, 2002.

20 Harrad, S., de Wit, C. A., Abdallah, M. A.-E., Bergh, C., Björklund, J. A., Covaci, A., Darnerud, P. O., de Boer, J., Diamond, M., and Huber, S.: Indoor contamination with hexabromocyclododecanes, polybrominated diphenyl ethers, and perfluoroalkyl compounds: an important exposure pathway for people?, *Environ. Sci. Technol.*, 44, 3221–3231, 2010.

Hoh, E. and Hites, R. A.: Brominated flame retardants in the atmosphere of the East-Central United States, *Environ. Sci. Technol.*, 39, 7794–7802, 2005.

25 International Commission on Radiological Protection, I.: ICRP Publication 66: Human Respiratory Tract Model for Radiological Protection, 66, Elsevier Health Sciences, New York, USA, 1995.

Kajiwara, N., Noma, Y., and Takigami, H.: Photolysis studies of technical decabromodiphenyl ether (DecaBDE) and ethane (DeBDethane) in plastics under natural sunlight, *Environ. Sci. Technol.*, 42, 4404–4409, 2008.

30 Kakimoto, K., Nagayoshi, H., Takagi, S., Akutsu, K., Konishi, Y., Kajimura, K., Hayakawa, K., and Toriba, A.: Inhalation and dietary exposure to Dechlorane Plus and polybrominated diphenyl ethers in Osaka, Japan, *Ecotoxicol. Environ. Saf.*, 99, 69–73, 2014.

[Title Page](#)[Abstract](#)[Introduction](#)[Conclusions](#)[References](#)[Tables](#)[Figures](#)[|◀](#)[▶|](#)[◀](#)[▶](#)[Back](#)[Close](#)[Full Screen / Esc](#)[Printer-friendly Version](#)[Interactive Discussion](#)

Kavouras, I. G., Lawrence, J., Koutrakis, P., Stephanou, E. G., and Oyola, P.: Measurement of particulate aliphatic and polynuclear aromatic hydrocarbons in Santiago de Chile: source reconciliation and evaluation of sampling artifacts, *Atmos. Environ.*, 33, 4977–4986, 1999.

Kawanaka, Y., Matsumoto, E., Sakamoto, K., Wang, N., and Yun, S. J.: Size distributions of 5 mutagenic compounds and mutagenicity in atmospheric particulate matter collected with a low-pressure cascade impactor, *Atmos. Environ.*, 38, 2125–2132, 2004.

Kemmlein, S., Herzke, D., and Law, R. J.: Brominated flame retardants in the European chemicals policy of REACH – regulation and determination in materials, *J. Chromatogr. A*, 1216, 320–333, 2009.

La Guardia, M. J., Hale, R. C., and Harvey, E.: Detailed polybrominated diphenyl ether (PBDE) 10 congener composition of the widely used penta-, octa-, and deca-PBDE technical flame-retardant mixtures, *Environ. Sci. Technol.*, 40, 6247–6254, 2006.

Larsen, R. K. and Baker, J. E.: Source apportionment of polycyclic aromatic hydrocarbons in the 15 urban atmosphere: a comparison of three methods, *Environ. Sci. Technol.*, 37, 1873–1881, 2003.

Lee, R. G. M., Thomas, G. O., and Jones, K. C.: PBDEs in the atmosphere of three locations in Western Europe, *Environ. Sci. Technol.*, 38, 699–706, 2004.

Li, P. F., Li, X., Yang, C. Y., Wang, X. J., Chen, J. M., and Collett, J. L.: Fog water chemistry in 20 Shanghai, *Atmos. Environ.*, 45, 4034–4041, 2011.

Li, X., Li, P., Yan, L., Chen, J., Cheng, T., and Xu, S.: Characterization of polycyclic aromatic 25 hydrocarbons in fog-rain events, *J. Environ. Monit.*, 13, 2988–2993, 2011.

Li, Y., Lin, T., Wang, F., Ji, T., and Guo, Z.: Seasonal variation of polybrominated diphenyl ethers in PM_{2.5} aerosols over the East China Sea, *Chemosphere*, 119, 675–681, 2015.

Lohmann, R. and Lammel, G.: Adsorptive and absorptive contributions to the gas-particle 30 partitioning of polycyclic aromatic hydrocarbons: state of knowledge and recommended parametrization for modeling, *Environ. Sci. Technol.*, 38, 3793–3803, 2004.

Lohmann, R., Gioia, R., Eisenreich, S. J., and Jones, K. C.: Assessing the importance of absorption and adsorption to the gas-particle partitioning of PCDD/Fs, *Atmos. Environ.*, 41, 7767–7777, 2007.

Luo, P., Bao, L.-J., Wu, F.-C., Li, S.-M., and Zeng, E. Y.: Health risk characterization for resident inhalation exposure to particle-bound halogenated flame retardants in a typical E-waste recycling zone, *Environ. Sci. Technol.*, 48, 8815–8822, 2014a.

Luo, P., Ni, H. G., Bao, L. J., Li, S. M., and Zeng, E. Y.: Size distribution of airborne particle-bound polybrominated diphenyl ethers and its implications for dry and wet deposition, *Environ. Sci. Technol.*, 48, 13793–13799, 2014b.

5 Lv, Y., Li, X., Xu, T. T., Cheng, T. T., Yang, X., Chen, J. M., Linuma, Y., and Herrmann, H.: Size distributions of polycyclic aromatic hydrocarbons in urban atmosphere: sorption mechanism and source contributions to respiratory deposition, *Atmos. Chem. Phys. Discuss.*, 15, 20811–20850, doi:10.5194/acpd-15-20811-2015, 2015.

10 Mandalakis, M., Besis, A., and Stephanou, E. G.: Particle-size distribution and gas/particle partitioning of atmospheric polybrominated diphenyl ethers in urban areas of Greece, *Environ. Pollut.*, 157, 1227–1233, 2009.

Marklund, A., Andersson, B., and Haglund, P.: Screening of organophosphorus compounds and their distribution in various indoor environments, *Chemosphere*, 53, 1137–1146, 2003.

15 Moller, A., Xie, Z. Y., Cai, M. H., Zhong, G. C., Huang, P., Cai, M. G., Sturm, R., He, J. F., and Ebinghaus, R.: Polybrominated diphenyl ethers vs. alternate brominated flame retardants and dechloranes from East Asia to the Arctic, *Environ. Sci. Technol.*, 45, 6793–6799, 2011.

Muenhor, D., Harrad, S., Ali, N., and Covaci, A.: Brominated flame retardants (BFRs) in air and dust from electronic waste storage facilities in Thailand, *Environ. Int.*, 36, 690–698, 2010.

20 Okonski, K., Degrendele, C., Melymuk, L., Landlova, L., Kukucka, P., Vojta, S., Kohoutek, J., Cupr, P., and Klanova, J.: Particle size distribution of halogenated flame retardants and implications for atmospheric deposition and transport, *Environ. Sci. Technol.*, 48, 14426–14434, 2014.

Pandis, S. N., Harley, R. A., Cass, G. R., and Seinfeld, J. H.: Secondary organic aerosol formation and transport, *Atmos. Environ.*, 26, 2269–2282, 1992.

25 Pankow, J. F.: Review and comparative-analysis of the theories on partitioning between the gas and aerosol particulate phases in the atmosphere, *Atmos. Environ.*, 21, 2275–2283, 1987.

Pankow, J. F.: An absorption-model of gas-particle partitioning of organic-compounds in the atmosphere, *Atmos. Environ.*, 28, 185–188, 1994a.

Pankow, J. F.: An absorption-model of the gas aerosol partitioning involved in the formation of secondary organic aerosol, *Atmos. Environ.*, 28, 189–193, 1994b.

30 Pankow, J. F. and Bidleman, T. F.: Interdependence of the slopes and intercepts from log log correlations of measured gas particle partitioning and vapor-pressure.1.Theory and analysis of available data, *Atmos. Environ.*, 26, 1071–1080, 1992.

[Title Page](#)

[Abstract](#)

[Introduction](#)

[Conclusions](#)

[References](#)

[Tables](#)

[Figures](#)

◀

▶

◀

▶

[Back](#)

[Close](#)

[Full Screen / Esc](#)

[Printer-friendly Version](#)

[Interactive Discussion](#)



PBDEs size distribution and health impact

Y. Lyu et al.

[Title Page](#)[Abstract](#)[Introduction](#)[Conclusions](#)[References](#)[Tables](#)[Figures](#)[|◀](#)[▶|](#)[◀](#)[▶](#)[Back](#)[Close](#)[Full Screen / Esc](#)[Printer-friendly Version](#)[Interactive Discussion](#)

Rudich, Y., Donahue, N. M., and Mentel, T. F.: Aging of organic aerosol: bridging the gap between laboratory and field studies, *Annu. Rev. Phys. Chem.*, 58, 321–352, 2007.

Söderström, G., Sellström, U., de Wit, C. A., and Tysklind, M.: Photolytic debromination of decabromodiphenyl ether (BDE 209), *Environ. Sci. Technol.*, 38, 127–132, 2004.

Shen, X., Zhao, Y., Chen, Z., and Huang, D.: Heterogeneous reactions of volatile organic compounds in the atmosphere, *Atmos. Environ.*, 68, 297–314, 2013.

Shi, J. and Cui, L. L.: Characteristics of high impact weather and meteorological disaster in Shanghai, China, *Nat. Hazards*, 60, 951–969, 2012.

Su, Y. S., Hung, H., Brice, K. A., Su, K., Alexandrou, N., Blanchard, P., Chan, E., Sverko, E., and Fellin, P.: Air concentrations of polybrominated diphenyl ethers (PBDEs) in 2002–2004 at a rural site in the Great Lakes, *Atmos. Environ.*, 43, 6230–6237, 2009.

Tian, M., Chen, S.-J., Wang, J., Zheng, X.-B., Luo, X.-J., and Mai, B.-X.: Brominated flame retardants in the atmosphere of E-waste and rural sites in Southern China: seasonal variation, temperature dependence, and gas-particle partitioning, *Environ. Sci. Technol.*, 45, 8819–8825, 2011.

Tittlemier, S. A., Halldorson, T., Stern, G. A., and Tomy, G. T.: Vapor pressures, aqueous solubilities, and Henry's law constants of some brominated flame retardants, *Environ. Toxicol. Chem.*, 21, 1804–1810, 2002.

Venkataraman, C., Thomas, S., and Kulkarni, P.: Size distributions of polycyclic aromatic hydrocarbons – gas/particle partitioning to urban aerosols, *J. Aerosol Sci.*, 30, 759–770, 1999.

Volckens, J. and Leith, D.: Effects of sampling bias on gas–particle partitioning of semi-volatile compounds, *Atmos. Environ.*, 37, 3385–3393, 2003.

Wang, J., Ho, S. S. H., Cao, J., Huang, R., Zhou, J., Zhao, Y., Xu, H., Liu, S., Wang, G., Shen, Z., and Han, Y.: Characteristics and major sources of carbonaceous aerosols in PM_{2.5} from Sanya, China, *Sci. Total Environ.*, 530–531, 110–119, 2015.

Wang, X. M., Ding, X., Mai, B. X., Xie, Z. Q., Xiang, C. H., Sun, L. G., Sheng, G. Y., Fu, J. M., and Zeng, E. Y.: Polybrominated diphenyl ethers in airborne particulates collected during a research expedition from the Bohai Sea to the Arctic, *Environ. Sci. Technol.*, 39, 7803–7809, 2005.

Wang, Z.-Y., Zeng, X.-L., and Zhai, Z.-C.: Prediction of supercooled liquid vapor pressures and n-octanol/air partition coefficients for polybrominated diphenyl ethers by means of molecular descriptors from DFT method, *Sci. Total Environ.*, 389, 296–305, 2008.

Wensing, M., Uhde, E., and Salthammer, T.: Plastics additives in the indoor environment – flame retardants and plasticizers, *Sci. Total Environ.*, 339, 19–40, 2005.

Wilford, B. H., Harner, T., Zhu, J. P., Shoeib, M., and Jones, K. C.: Passive sampling survey of polybrominated diphenyl ether flame retardants in indoor and outdoor air in Ottawa, Canada: implications for sources and exposure, *Environ. Sci. Technol.*, 38, 5312–5318, 2004.

Yang, M., Jia, H. L., Ma, W. L., Qi, H., Cui, S., and Li, Y. F.: Levels, compositions, and gas-particle partitioning of polybrominated diphenyl ethers and dechlorane plus in air in a Chinese northeastern city, *Atmos. Environ.*, 55, 73–79, 2012.

Yang, M., Qi, H., Jia, H. L., Ren, N. Q., Ding, Y. S., Ma, W. L., Liu, L. Y., Hung, H., Sverko, E., and Li, Y. F.: Polybrominated diphenyl ethers in air across China: levels, compositions, and gas-particle partitioning, *Environ. Sci. Technol.*, 47, 8978–8984, 2013.

Yu, H. and Yu, J. Z.: Polycyclic aromatic hydrocarbons in urban atmosphere of Guangzhou, China: size distribution characteristics and size-resolved gas-particle partitioning, *Atmos. Environ.*, 54, 194–200, 2012.

Yu, Z., Liao, R., Li, H., Mo, L., Zeng, X., Sheng, G., and Fu, J.: Particle-bound Dechlorane Plus and polybrominated diphenyl ethers in ambient air around Shanghai, China, *Environ. Pollut.*, 159, 2982–2988, 2011.

Zhang, B. Z., Guan, Y. F., Li, S. M., and Zeng, E. Y.: Occurrence of Polybrominated Diphenyl Ethers in Air and Precipitation of the Pearl River Delta, South China: annual Washout Ratios and Depositional Rates, *Environ. Sci. Technol.*, 43, 9142–9147, 2009.

Zhang, B. Z., Zhang, K., Li, S. M., Wong, C. S., and Zeng, E. Y.: Size-dependent dry deposition of airborne polybrominated diphenyl ethers in urban Guangzhou, China, *Environ. Sci. Technol.*, 46, 7207–7214, 2012.

Zhang, K., Zhang, B. Z., Li, S. M., Wong, C. S., and Zeng, E. Y.: Calculated respiratory exposure to indoor size-fractionated polycyclic aromatic hydrocarbons in an urban environment, *Sci. Total Environ.*, 431, 245–251, 2012.

Zielinska, B., Sagebiel, J., Arnott, W. P., Rogers, C. F., Kelly, K. E., Wagner, D. A., Lighty, J. S., Sarofim, A. F., and Palmer, G.: Phase and size distribution of polycyclic aromatic hydrocarbons in diesel and gasoline vehicle emissions, *Environ. Sci. Technol.*, 38, 2557–2567, 2004.

PBDEs size distribution and health impact

Y. Lyu et al.

Title Page

Abstract

Introduction

Conclusions

References

Tables

Figures

◀

▶

◀

▶

Back

Close

Full Screen / Esc

Printer-friendly Version

Interactive Discussion



Table 1. Physiochemical properties of the target PBDE congeners and data from Yang et al. (2013).

Chemical	Molecule	MW ^a	log p_L^o (Pa) ^b	log K_{OA}^c	Gas phase ^e (pg m^{-3})	Particulate phase ^e (pg m^{-3})
BDE-17	2,2',4-tribromodiphenyl ether	406.9	-2.71 ^d	9.31	15.64	0.93
BDE-28	2,4,4'-tribromodiphenyl ether	406.9	-2.95	9.4	30.04	1.17
BDE-71	2,3',4',6-tetrabromodiphenyl ether	485.8	-3.55 ^d	10.2		
BDE-47	2,2',4,4'-tetrabromodiphenyl ether	485.8	-4.07	10.1	28.81	5.38
BDE-66	2,3',4,4'-tetrabromodiphenyl ether	485.8	-4.27	10.25	6.11	0.38
BDE-100	2,2',4,4',6-pentabromodiphenyl ether	564.7	-4.91	10.82	3.38	1.52
BDE-99	2,2',4,4',5-pentabromodiphenyl ether	564.7	-5.14	10.96	8.02	5.06
BDE-85	2,2',3,4,4'-pentabromodiphenyl ether	564.7	-5.40	11.03	2.58	2.42
BDE-154	2,2',4,4',5,6'-hexabromodiphenyl ether	643.6	-5.83	11.66	1.37	2.10
BDE-153	2,2',4,4',5,5'-hexabromodiphenyl ether	643.6	-6.08	11.77	1.27	2.39
BDE-138	2,2',3,4,4',5'-hexabromodiphenyl ether	643.6	-6.23	11.81	1.09	2.21
BDE-183	2,2',3,4,4',5',6-heptabromodiphenyl ether	722.5	-6.75	12.52	1.67	10.01
BDE-190	2,3,3',4,4',5,6-heptabromodiphenyl ether	722.5	-7.00	12.71		

^a Molecular weight.^b Subcooled liquid vapor pressure in 292 K from Tittlemier et al. (2002).^c Octanol-air partition coefficient in 292 K from Harner and Shoeib (1998).^d data from Wang et al. (2008).^e data from Yang et al. (2013).

Title Page

Abstract

Introduction

Conclusions

References

Tables

Figures

|◀

▶|

◀

▶

Back

Close

Full Screen / Esc

Printer-friendly Version

Interactive Discussion



PBDEs size distribution and health impact

Y. Lyu et al.

Table 2. A_{TSP} and f_{OM} adopted from Yu and Yu (2012).

μm	< 0.4	0.4–0.7	0.7–1.1	1.1–2.1	2.1–3.3	3.3–4.7	4.7–5.8	5.8–9	9–10
$A_{\text{TSP}} (\text{m}^2 \text{g}^{-1})$	50	10	10	19	19	19	19	19	19
f_{OM}	0.45	0.35	0.35	0.25	0.25	0.25	0.25	0.25	0.25

[Title Page](#)[Abstract](#)[Introduction](#)[Conclusions](#)[References](#)[Tables](#)[Figures](#)[|◀](#)[▶|](#)[◀](#)[▶](#)[Back](#)[Close](#)[Full Screen / Esc](#)[Printer-friendly Version](#)[Interactive Discussion](#)

Table 3. Seasonal concentrations of size-resolved particulate PBDEs in urban Shanghai (pg m^{-3}).

Compound	Spring		Summer		Autumn		Winter	
	Mean	Range	Mean	Range	Mean	Range	Mean	Range
BDE-17	nd	nd–0.37	0.08	nd–0.27	0.11	nd–0.52	0.10	nd–0.46
BDE-28	nd	nd–0.18	nd	nd–0.13	nd	nd–0.18	0.11	nd–0.68
BDE-71	nd	nd–0.17	nd	nd–0.18	nd	nd–0.19	nd	nd–0.93
BDE-47	0.48	0.24–0.82	0.57	0.35–1.12	0.44	0.24–0.80	0.38	0.11–1.16
BDE-66	nd	nd–0.16	nd	nd–0.19	nd	nd	0.16	nd–1.46
BDE-100	nd	nd	nd	nd	nd	nd	nd	nd–0.23
BDE-99	3.28	1.27–6.73	1.74	1.01–7.10	4.14	0.63–8.29	4.74	1.61–12.4
BDE-85	2.38	0.78–7.15	1.12	0.31–3.06	2.31	0.45–4.50	3.54	0.81–12.2
BDE-154	nd	nd–2.85	nd	nd–0.42	nd	nd	nd	nd–2.85
BDE-153	1.08	nd–3.07	0.44	nd–2.40	0.42	nd–2.15	1.29	nd–5.43
BDE-138	1.05	0.30–2.85	0.46	nd–2.19	1.20	0.34–2.15	1.18	0.29–2.89
BDE-183	0.65	nd–0.78	nd	nd–0.67	0.72	nd–1.12	0.81	nd–1.25
BDE-190	nd	nd–0.91	nd	nd	nd	nd–0.76	nd	nd–0.96
$\Sigma_{13}\text{PBDE}$	90.3	76.3–106	52.6	30.6–82.2	93.9	90.7–100	117	104–141

nd = not detected.

[Title Page](#)[Abstract](#)[Introduction](#)[Conclusions](#)[References](#)[Tables](#)[Figures](#)[◀](#)[▶](#)[◀](#)[▶](#)[Back](#)[Close](#)[Full Screen / Esc](#)[Printer-friendly Version](#)[Interactive Discussion](#)

Table 4. Pearson correlation matrix for the concentrations of PBDE congeners.

	BDE-17	BDE-28	BDE-71	BDE-47	BDE-66	BDE-100	BDE-99	BDE-85	BDE-154	BDE-153	BDE-138	BDE-183	BDE-190
BDE-17	1	0.75^b	0.45^a	0.18	-0.11	0.69^b	0.18	0.38	-0.11	-0.16	0.11	0.39	0.16
BDE-28		1	0.65^b	-0.05	0.39	0.69^b	0.45^a	0.69^b	-0.16	0.05	0.04	0.28	0.15
BDE-71			1	0.16	0.27	0.82^b	0.60^b	0.70^b	-0.06	0.34	0.31	0.18	0.48^a
BDE-47				1	0.01	0.36	-0.22	-0.19	0.08	-0.27	-0.08	0.24	0.71^b
BDE-66					1	0.27	0.30	0.51^a	0.26	0.18	-0.10	-0.06	0.25
BDE-100						1	0.54^a	0.67^b	0.11	0.13	0.22	0.19	0.57^b
BDE-99							1	0.83^b	0.14	0.37	0.68^b	0.30	0.41
BDE-85								1	0.18	0.37	0.44^a	0.21	0.37
BDE-154									1	0.35	0.34	0.20	0.19
BDE-153										1	0.56^b	-0.07	0.09
BDE-138											1	0.47^a	0.37
BDE-183												1	0.28
BDE-190													1

Significant values are marked in bold.

^a Correlation is significant at 0.05 level (2-tailed).

^b Correlation is significant at 0.01 level (2-tailed).

Title Page	Abstract	Introduction
Conclusions	References	
Tables	Figures	
◀	▶	
◀	▶	
Back	Close	
Full Screen / Esc		
Printer-friendly Version		
Interactive Discussion		



PBDEs size distribution and health impact

Y. Lyu et al.

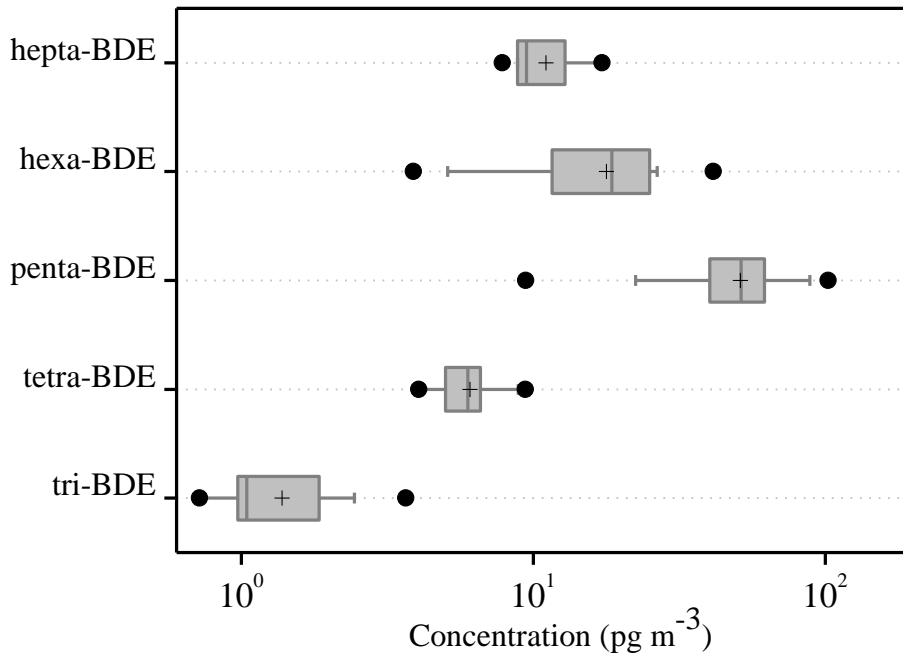


Figure 1. Concentration profiles of PBDE homologue groups in urban atmosphere. Solid vertical lines and the horizontal lines represent median and mean values, respectively. Box plots represent 25th–75th percentiles, whereas whiskers indicate 5th and 95th percentile. The solid spheres crosses represent maximum and minimum values.

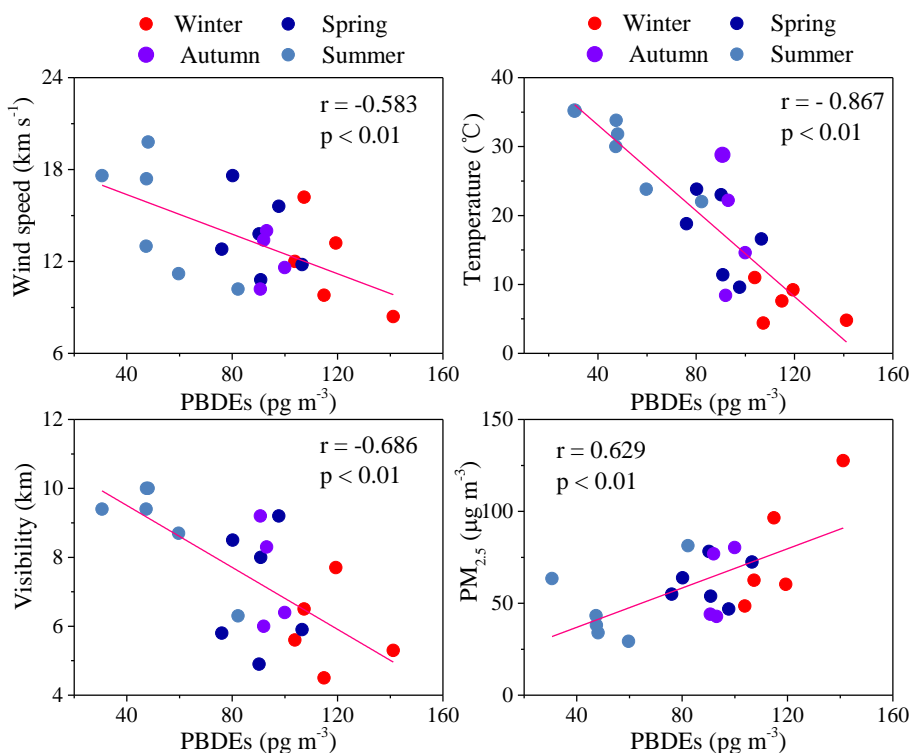


Figure 2. Pearson correlation between particulate PBDEs and weather parameters: visibility, temperature, wind speed and PM_{2.5}.

PBDEs size distribution and health impact

Y. Lyu et al.

Title Page

Abstract

Introduction

Conclusions

References

Tables

Figures

◀

▶

Back

Close

Full Screen / Esc

Printer-friendly Version

Interactive Discussion

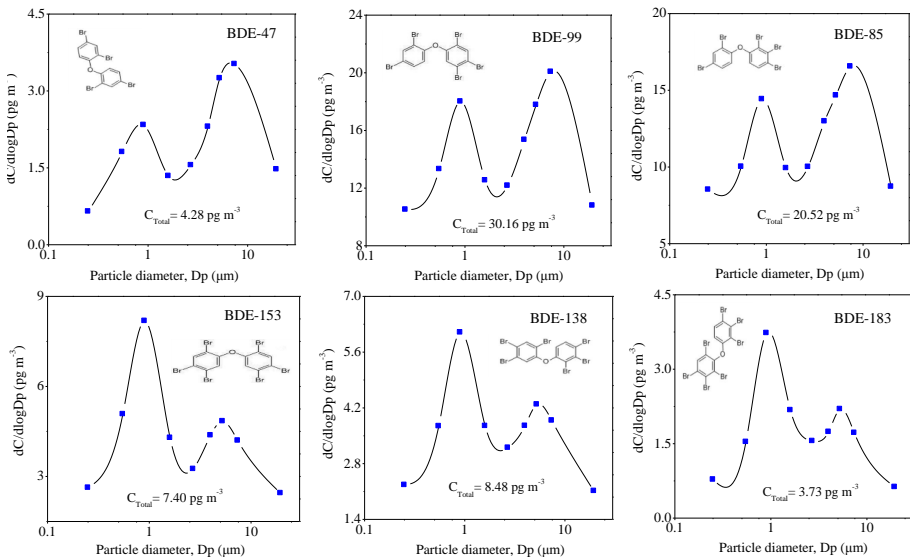


Figure 3. Mean normalized particle-size distribution of PBDE congeners for all samples. dC is the concentration on each filter, C is the sum concentration on all filters, and $d\log D_p$ is the logarithmic size interval for each impactor stage in particle diameter (D_p).

PBDEs size distribution and health impact

Y. Lyu et al.

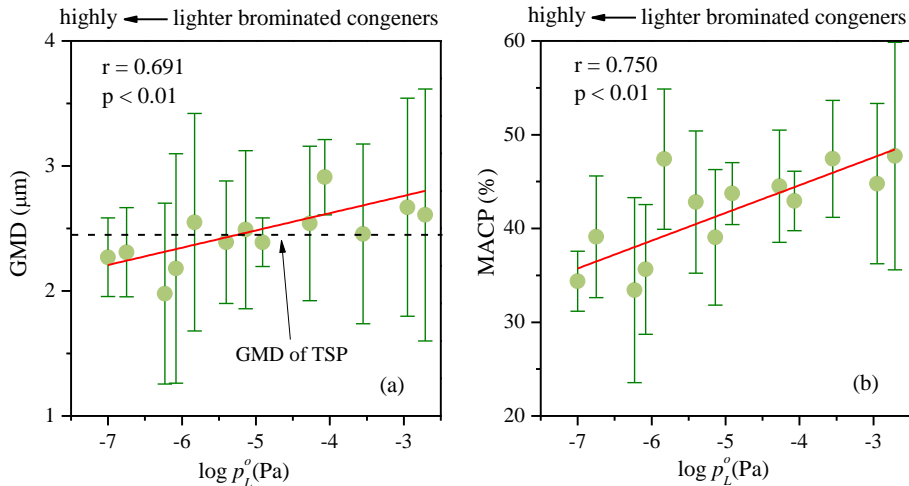


Figure 4. Pearson correlation between GMD and $\log p_L^o$ of all particulate PBDEs (left) as well as between MFCP and $\log p_L^o$ (right) at 292 K.

Title Page
Abstract
Conclusions
Tables
◀
◀
Back
Full Screen / Esc

Introduction
References
Figures
▶
▶
Close
Printer-friendly Version
Interactive Discussion



PBDEs size distribution and health impact

Y. Lyu et al.

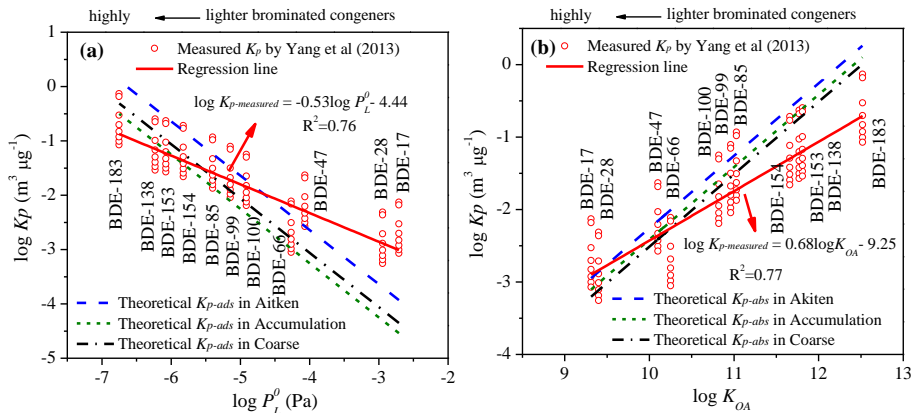
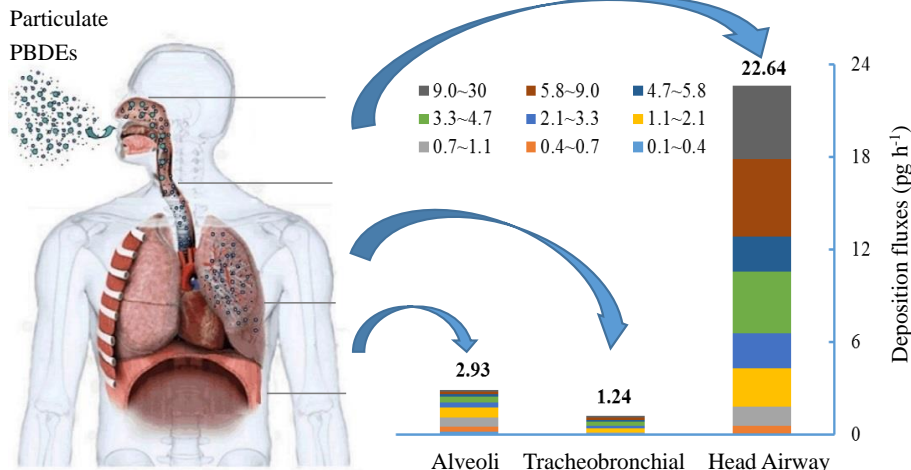


Figure 5. Comparison of theoretical K_p based on adsorption (a) and absorption (b) in three modes with measured K_p values by Yang et al. (2013) in Shanghai from 2008 to 2009.

PBDEs size distribution and health impact

Y. Lyu et al.

**Figure 6.** Deposition fluxes of size-resolved particulate PBDEs in human respiratory tract.

PBDEs size distribution and health impact

Y. Lyu et al.

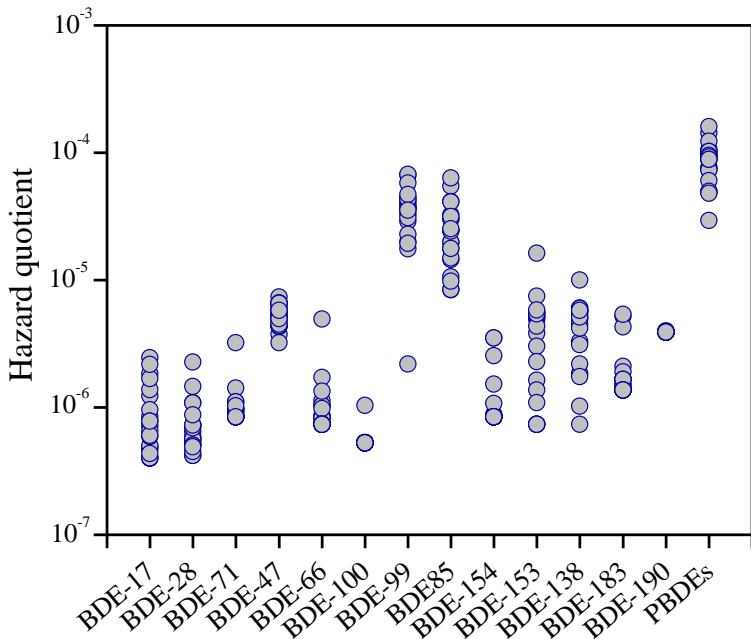


Figure 7. Hazard quotient (HQ) for particulate PBDEs in Shanghai atmosphere. PBDEs is the sum of BDE-17, 28, 71, 47, 66, 100, 99, 85, 154, 153, 138, 183, and 190.

PBDEs size distribution and health impact

Y. Lyu et al.

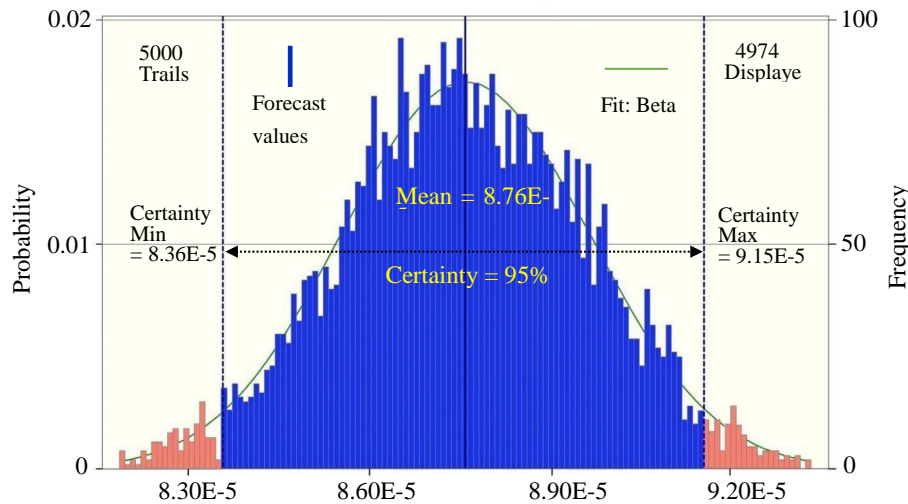


Figure 8. Probability distributions of hazard quotient of PBDEs in Monte Carlo simulations with five thousand trials.

- [Title Page](#)
- [Abstract](#) [Introduction](#)
- [Conclusions](#) [References](#)
- [Tables](#) [Figures](#)
- [◀](#) [▶](#)
- [◀](#) [▶](#)
- [Back](#) [Close](#)
- [Full Screen / Esc](#)
- [Printer-friendly Version](#)
- [Interactive Discussion](#)